Available online at www.sciencedirect.com
ScienceDirect
International Journal of Heat and Mass Transfer 51 (2008) 630–639
International Journal of HEAT and MASS TRANSFER
www.elsevier.com/locate/ijhmt

Forced oscillation in diffusion flames near diffusive–thermal resonance

H.Y. Wang [a], J.K. Bechtold [b], C.K. Law [a,*]

[a] Department of Mechanical and Aerospace Engineering, Princeton University, Princeton, NJ 08544, USA
[b] Department of Mathematical Sciences, New Jersey Institute of Technology, Newark, NJ 07102, USA

Received 21 August 2006; received in revised form 29 April 2007
Available online 16 July 2007

Abstract

In this work, we carry out a systematic analysis of forced oscillation in planar diffusion flames under weak external forcing. The external forcing is introduced by independently imposing a flow field with small amplitude fluctuations. Employing the asymptotic theory of Cheatham and Matalon, the linear response is first examined. It is shown that when the Damköhler number Da is close to the critical value Da^* corresponding to the marginal state of diffusive–thermal pulsating instability, the imposed velocity fluctuation may induce very large amplitude of flame oscillation as the frequency of velocity fluctuation c approaches c_0, the flame oscillation frequency at the onset of instability. This is a resonance phenomenon between the imposed flow oscillations and the intrinsic flame oscillations that are driven by the diffusive–thermal instability, and hence we refer to this as the diffusive–thermal resonance. The nonlinear near-resonant response is then examined with the Damköhler number Da chosen to be very close to the critical Damköhler number Da^*, and we derive an evolution equation for the amplitude of forced oscillation. Examination of the evolution equation reveals that in most situations, flames with larger Lewis number of fuel, smaller initial mixture strength, and smaller temperature difference between the oxidant and fuel stream are more responsive to the external forcing.

Keywords: Diffusion flame; Forced oscillation; Pulsating instability; Linear response; Nonlinear response

1. Introduction

Flames in practical combustors are subjected to fluctuating flows imposed by the random motion of eddies whose wide spectrum of length and time scales may interact with the flames in very different ways. Since a direct study of the flame response to flow unsteadiness in turbulent combustion is rather complicated, the effect of flow unsteadiness on laminar flames has received considerable attention for its potential application to the fundamental understanding and modeling of turbulent combustion through the concept of laminar flamelets [1].

Unsteady effects on both diffusion and premixed flames have been studied with emphasis on the dynamic response to oscillatory strain rate variations. In particular, results on diffusion flames [2–14] show that the flame response becomes more sensitive to the imposed unsteadiness when the otherwise steady flame is near its extinction limit; whereas the response for flames far from extinction is attenuated monotonically as the frequency of the imposed oscillation increases. Consequently, unsteady flames can withstand higher strain rates at higher frequencies than at lower frequencies. However, there have been relatively few previous theoretical investigations. Strahle [2] studied the convective droplet burning at a stagnation point under the influence of small amplitude sound wave from the free stream. Im et al. [13,14] analyzed the response of counterflow diffusion flames to monochromatic oscillatory strain rates using large activation energy asymptotics, with attention focused on near extinction conditions so that the time scale of the imposed unsteadiness is comparable to that of diffusive transport. The results of Im et al. [13] suggest that the unsteady characteristics of the near-extinction diffusion

* Corresponding author. Tel.: +1 (10) 609 258 5271; fax: +1 (10) 609 258 6233.
E-mail address: cklaw@princeton.edu (C.K. Law).

0017-9310/$ - see front matter © 2007 Elsevier Ltd. All rights reserved.
doi:10.1016/j.ijheatmasstransfer.2007.04.042

Nomenclature

A	amplitude function
c_0	frequency at the onset of intrinsic oscillation
Da	Damköhler number
Da^*	Damköhler number at the onset of instability
h_j^*	excess/deficiency enthalpy for species j, $j = F, O$
Le_j	Lewis number of species j, $j = F, O$
R	modulus of amplitude function A
S_j	leakage function for species j, $j = F, O$
t	fast time
T	temperature
u	response of temperature to external forcing
v	response of fuel mass fraction to external forcing
w	response of oxidant mass fraction to external forcing
x_f	location of flame surface
Y_F	fuel mass fraction
Y_O	oxidant mass fraction

Greek symbols

β	Zeldovich number
δ	reduced Damköhler number
ϕ	initial mixture strength
γ	heat transfer parameter
θ	polar angle of amplitude function A
τ_1, τ_2	slow time variables
ξ_f	location of stoichiometric flame surface
λ_J	$\frac{1}{2}\sqrt{Le_J^2 + 4iLe_Jc},\ J = T, F, O$
λ_J	$\frac{1}{2}\sqrt{Le_J^2 + 4iLe_Jc_0},\ J = T, F, O$
μ_J	$\frac{1}{2}\sqrt{Le_J^2 + 8iLe_Jc_0},\ J = T, F, O$

Subscripts and superscripts

b	basic state quantity
p	particular solution to the flame responses
F	fuel
O	oxidant
$-\infty$	fuel boundary
∞	oxidant boundary
$+$	oxidant side of flame sheet
$-$	fuel side of flame sheet

flame can be significantly different from those in the Burke–Schumann limit.

These earlier studies, however, have not addressed the important issue of resonance. That is, combustion systems may exhibit intrinsic oscillation of different modes and those oscillations may then interact with the imposed flow oscillations so that the flame responses could be significantly different. For example, recent studies have shown that, when the Lewis numbers of the reactants are sufficiently larger than unity, intrinsic oscillations due to the imbalance of thermal and mass diffusions, referred to as the thermal–diffusive pulsating instability, may develop near but prior to extinction, leading eventually to flame quenching [15–18]. Thus, such unstable diffusion flames could extinguish at a larger Damköhler number, denoted as the dynamic extinction Damköhler number, Da^*, than the static extinction Damköhler number, Da_{ext}.

The primary objective of the present study is therefore to analyze the flame response to external forcing coupled with intrinsic flame oscillations. Specifically, we consider the simple geometric configuration of a planar diffusion flame situated in a channel at the interface between a fuel being supplied from below with a velocity field with harmonic fluctuation of small amplitude, and an oxidant diffusing in from a cross-stream above. This configuration eliminates the effect of strain rate so that the flame is only subjected to the unsteadiness of the velocity field. Intrinsic oscillation of the planar diffusion flame due to thermal–diffusive instability is considered. The Lewis numbers for both the fuel and oxidant are assumed to be larger than unity and focus our attention on the flame response near the dynamic extinction limit, Da^*, instead of the static extinction limit, Da_{ext}, considered in previous studies. We carry out a systematic analysis on the linear and nonlinear response of the flame oscillation subjected to small amplitude, harmonic velocity fluctuation by employing the asymptotic theory of Cheatham and Matalon [19]. The linear response shows that the resonance phenomena may occur as the frequency of velocity fluctuation approaches the intrinsic oscillation frequency when the flame is near the stability boundary. The nonlinear near-resonant response is then analyzed by deriving an evolution equation for the amplitude of forced oscillation. The Damköhler number Da and forced frequency c are chosen to be close to Da^* and the intrinsic oscillation frequency, c_0, so that even very weak forcing is able to induce rather large oscillation amplitude. It is shown that by considering the inherent nonlinearity, the flame oscillation exhibits finite amplitude at the resonant condition.

2. Formulation

We consider the simple configuration of a planar flame in a chamber [18,19]. As shown in Fig. 1, the fuel stream is fed from the bottom of the chamber and the oxidant diffuses against the fuel stream from a fast cross-stream at the top of the chamber. We employ the asymptotic theory of Cheatham and Matalon [19] in which the convective–diffusive equations for temperature and fuel and oxidant mass fractions are solved on either side of the flame surface, x_f.

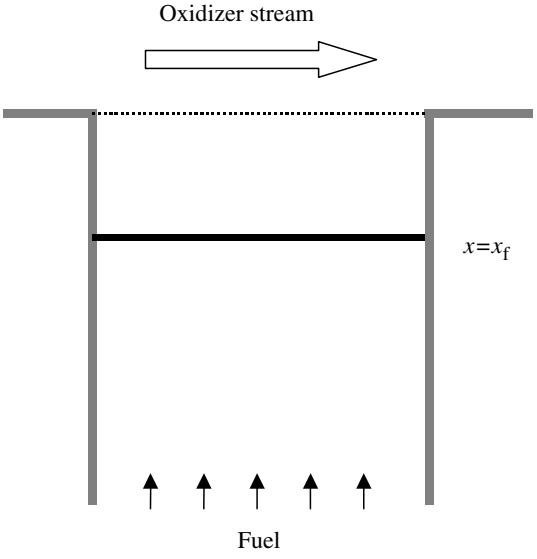

Fig. 1. The one-dimensional chambered flame configuration.

These quantities are then related across the flame using the jump relations obtained by asymptotic analysis of the reaction zone. Assuming constant physical and chemical properties of reactants, constant density, and one-step irreversible chemical reaction, the appropriate non-dimensional governing equations can be written as [19]:

$$\frac{\partial T}{\partial t}+U\frac{\partial T}{\partial x}-\frac{\partial^2 T}{\partial x^2}=0, \tag{1}$$

$$\frac{\partial Y_F}{\partial t}+U\frac{\partial Y_F}{\partial x}-\frac{1}{Le_F}\frac{\partial^2 Y_F}{\partial x^2}=0, \tag{2}$$

$$\frac{\partial Y_O}{\partial t}+U\frac{\partial Y_O}{\partial x}-\frac{1}{Le_O}\frac{\partial^2 Y_O}{\partial x^2}=0, \tag{3}$$

where T is the temperature, Y_F and Y_O the mass fractions of the fuel and oxidant, respectively, and Le_F and Le_O their corresponding Lewis numbers. The unsteadiness is introduced by independently imposing harmonic velocity fluctuation of small amplitude onto the unity mean velocity field. Thus, the velocity U is expressed as:

$$\begin{aligned} U &= 1+\beta^{-1}\varepsilon H(t),\\ H(t) &= h\exp(\mathrm{i}ct)+\text{c.c.}, \end{aligned} \tag{4}$$

where β is the Zel'dovich number, ε a small parameter satisfying $\beta^{-1}\ll\varepsilon\ll 1$, h the amplitude of velocity fluctuation, c the forced frequency and c.c. denotes the complex conjugate.

The boundary conditions are:

$$T=T_{-\infty},\quad Y_F=1,\quad Y_O=0\quad \text{as}\quad x\to-\infty, \tag{5}$$

$$T=T_{-\infty}+\Delta T,\quad Y_F=0,\quad Y_O=\phi^{-1}\quad \text{at}\quad x=0, \tag{6}$$

where ΔT is the temperature difference between the oxidant and fuel stream, and ϕ is the initial mixture strength, defined as the ratio of the fuel mass fraction at the fuel boundary to the oxidant mass fraction at the oxidant boundary, normalized by the mass-weighted stoichiometric coefficient ratio.

The jump relations at the reaction sheet location, x_f, are [19]:

$$[T]=[Y_F]=[Y_O]=0, \tag{7}$$

$$\left[\frac{\partial T}{\partial x}\right]=-\frac{1}{Le_F}\left[\frac{\partial Y_F}{\partial x}\right]=-\frac{1}{Le_O}\left[\frac{\partial Y_O}{\partial x}\right]. \tag{8}$$

Here we have adopted the notation $[T]=T^+(x_f)-T^-(x_f)$ and the superscripts "+/−" denote the solutions at the oxidant/fuel sides of the reaction sheet. Expressions for the amount of leakage of the reactants through the reaction sheet are given as [19]:

$$Y_F^+|_{x=x_f}=\beta^{-1}Le_F S_F(\gamma,\delta), \tag{9}$$

$$Y_O^-|_{x=x_f}=\beta^{-1}Le_O S_O(\gamma,\delta), \tag{10}$$

where the approximate formulas for the quantities S_F and S_O have been determined through curve fitting and are given in Refs. [18,19]. They depend only on two parameters γ and δ, where

$$\gamma=-\left(\left.\frac{\partial T^-}{\partial x}\right|_{x_f}+\left.\frac{\partial T^+}{\partial x}\right|_{x_f}\right)\Big/\left(\left.\frac{\partial T^-}{\partial x}\right|_{x_f}-\left.\frac{\partial T^+}{\partial x}\right|_{x_f}\right) \tag{11}$$

represents the excess of heat conducted away to one side of the reaction sheet from the total heat generated by the chemical reaction, and

$$\delta=4Le_F Le_O Da\left[\frac{\partial T}{\partial x}\right]^{-2}\exp\left(\frac{1+\gamma}{2}h_O^*+\frac{1-\gamma}{2}h_F^*\right) \tag{12}$$

is the reduced Damköhler number, which measures the intensity of the chemical reaction, and

$$h_F^*=T_1^++\frac{1}{Le_F}Y_{F,1}^+,\quad h_O^*=T_1^-+\frac{1}{Le_O}Y_{O,1}^-$$

are the excess/deficiency in the fuel and oxidant enthalpies, respectively, evaluated at the reaction sheet. Furthermore,

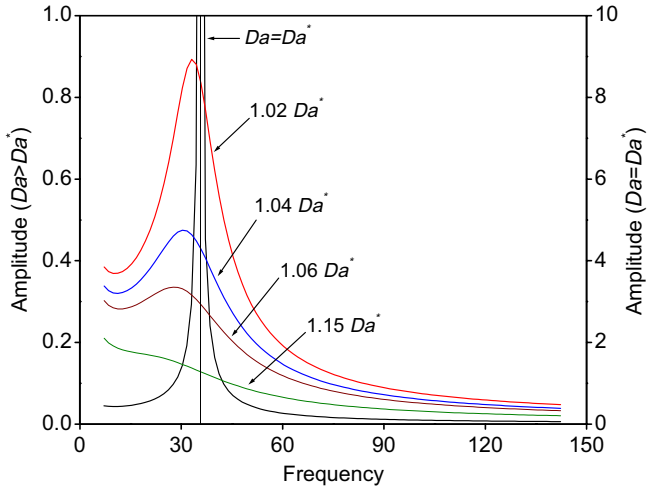

Fig. 2. Amplitude of u_p^+ versus forced frequency c for different values of Da (with $Le_F=2$, $Le_O=2$, $\phi=1$ and $\Delta T=0$).

subscript "1" denotes the $O(\beta^{-1})$ expression in a power series expansion in terms of β^{-1}.

S_F and S_O only have solutions when $\delta \geqslant \delta_c$, and for each $\delta > \delta_c$ there exist two distinct solutions characterized by different extents of reactant leakage (see, for example, Fig. 2 in Ref. [18]). The critical value δ_c depends only on γ and was determined by Liñán [20] as:

$$\delta_c = e\left\{(1-|\gamma|) - (1-|\gamma|)^2 + 0.26(1-|\gamma|)^3 + 0.055(1-|\gamma|)^4\right\}.$$

3. Linear response

A linear analysis is first conducted by assuming $h = 1$ such that the velocity fluctuation is of $O(\beta^{-1}\varepsilon)$ relative to its mean value, as shown in Eq. (4). The solution under a harmonic fluctuating velocity field (4) can be written in the form of steady-state base solutions for temperature, mass fractions of fuel and oxidant, and the flame sheet location under unity flow field plus a correction term accounting for the small velocity fluctuation:

$$T = T_b(x) + \beta^{-1}\varepsilon u(x,t) \tag{13}$$

$$Y_F = Y_{F,b}(x) + \beta^{-1}\varepsilon v(x,t) \tag{14}$$

$$Y_O = Y_{O,b}(x) + \beta^{-1}\varepsilon w(x,t) \tag{15}$$

$$x_f = x_{f,b} + \beta^{-1}\varepsilon l(x,t) \tag{16}$$

where u, v, w, and l are the correction terms for temperature, mass fractions of fuel and oxidant, and flame sheet location, respectively, and the base solutions T_b, $Y_{F,b}$, $Y_{O,b}$, and $x_{f,b}$ are respectively given by [19]:

$$T_b = \begin{cases} T_{-\infty} + (e^{-\xi_f} + \Delta T - 1)e^x \\ \quad + \frac{1}{\beta}\left\{\frac{Le_F}{Le_O}\frac{(1-e^{Le_O\xi_f}) - Le_O(1-e^{\xi_f})}{1-e^{Le_F\xi_f}} - \frac{S_O}{S_F}\right\}S_F e^{x-\xi_f}, & x < x_f \\ T_{-\infty} + 1 + (\Delta T - 1)e^x \\ \quad - \frac{1}{\beta}\left\{\frac{1-e^x}{1-e^{Le_F\xi_f}}\right\}Le_F S_F, & x > x_f, \end{cases}$$

$$Y_{F,b} = \begin{cases} 1 - e^{Le_F(x-\xi_f)} \\ \quad + \frac{1}{\beta}\left\{1 - \frac{Le_F}{Le_O}\frac{1-e^{Le_O\xi_f}}{1-e^{Le_F\xi_f}} + \frac{S_O}{S_F}\right\}Le_F S_F e^{Le_F(x-\xi_f)}, & x < x_f \\ \frac{1}{\beta}\left\{\frac{1-e^{Le_F x}}{1-e^{Le_F\xi_f}}\right\}Le_F S_F, & x > x_f, \end{cases}$$

$$Y_{O,b} = \begin{cases} \frac{1}{\beta}Le_O S_O e^{Le_O(x-\xi_f)}, & x < x_f \\ (1+\phi^{-1})e^{Le_O x} - 1 + \frac{1}{\beta}\left\{\frac{1-e^{Le_O x}}{1-e^{Le_F\xi_f}}\right\}Le_F S_F, & x > x_f, \end{cases}$$

$$x_{f,b} = \xi_f + \frac{1}{\beta}\left(S_O - \frac{Le_F}{Le_O}\frac{1-e^{Le_O\xi_f}}{1-e^{Le_F\xi_f}}S_F\right),$$

where ξ_f corresponds to the flame surface in the Burke–Schumann limit and is given by:

$$\xi_f = -Le_O^{-1}\ln(1+\phi^{-1}).$$

We note that the unsteady fluctuations induced by the perturbed flow field (4) are of $O(\beta^1\varepsilon)$. The magnitude of these terms is sufficient to elicit an O(1) response due to the extreme sensitivity of the Arrhenius reaction rate term.

Substituting Eqs. (13)–(16) into the governing Eqs. (1)–(3) for T, Y_F and Y_O and their boundary conditions, jump and leakage conditions (5)–(10) yields the governing equations for u, v and w:

$$u_t + u_x - u_{xx} = -\varepsilon(T_0)_x \exp(ict) + \text{c.c.}, \tag{17}$$

$$v_t + v_x - Le_F^{-1}v_{xx} = -\varepsilon(Y_{F,0})_x \exp(ict) + \text{c.c.}, \tag{18}$$

$$w_t + w_x - Le_O^{-1}w_{xx} = -\varepsilon(Y_{O,0})_x \exp(ict) + \text{c.c.}, \tag{19}$$

and their boundary conditions

$$u = v = w = 0 \text{ at } \quad x = 0 \text{ and as } \quad x \to -\infty, \tag{20}$$

jump relations

$$[u] = -Le_F^{-1}[v] = -Le_O^{-1}[w], \tag{21}$$

$$\left[u - \frac{\partial u}{\partial x}\right] = -\left[v - Le_F^{-1}\frac{\partial v}{\partial x}\right] = -\left[w - Le_O^{-1}\frac{\partial w}{\partial x}\right], \tag{22}$$

and leakage conditions

$$\varepsilon Le_F^{-1}v^+ = \sum_{k=1}^{\infty}\frac{1}{k!}\frac{\partial^k S_F(\gamma,\delta_b)}{\partial\delta_b^k}(\delta-\delta_b)^k, \tag{23}$$

$$\varepsilon Le_O^{-1}w^- = \sum_{k=1}^{\infty}\frac{1}{k!}\frac{\partial^k S_O(\gamma,\delta_b)}{\partial\delta_b^k}(\delta-\delta_b)^k, \tag{24}$$

where T_0, $Y_{F,0}$ and $Y_{O,0}$ are the leading-order base solutions in terms of β^{-1}, δ_b is the reduced Damköhler number evaluated at the steady-state condition and the subscript "x" denotes differentiation with respect to x. Eqs. (17)–(19) imply that the flame oscillates under the external harmonic driving force due to the velocity fluctuation.

The solutions to u, v and w assume the form

$$\phi(x,t) = \phi_p(x)\exp(ict) + \text{c.c.} + \phi_c(x)\exp(\sigma t),$$
$$\phi = u, v, w,$$

where the particular solution $\phi_p(x)\exp(ict) + c.c.$ accounts for the response to the velocity fluctuation and the common solution $\phi_c(x)\exp(\sigma t)$ is associated with the intrinsic instability. σ is a complex number whose real part identifies the growth rate. The Damköhler number Da of interest here is larger than its critical value Da^* corresponding to the marginal state of intrinsic instability. Thus, the flame is intrinsically stable so that the common solution $\phi_c(x)\exp(\sigma t)$ will damp out eventually, and hereafter, only the particular solution $\phi_p(x)\exp(ict) + c.c.$ is considered. It should be noted that $u_p(x)$, $v_p(x)$ and $w_p(x)$ are complex functions whose modulus denote the oscillation amplitude while the phase angle denotes the phase shift of oscillation from the imposed velocity fluctuation. The solutions to $u_p(x)$, $v_p(x)$ and $w_p(x)$ are

$$u_p(x) = \begin{cases} B_1\exp[(1/2+\Lambda_T)x] + \frac{i}{c}(e^{-\xi_f} + \Delta T - 1)e^x, & x < x_f \\ B_2\{\exp[(1/2+\Lambda_T)x] - \exp[(1/2-\Lambda_T)x]\} \\ \quad + \frac{i}{c}(\Delta T - 1)\{e^x - \exp[(1/2-\Lambda_T)x]\}, & x > x_f, \end{cases}$$

$$v_p(x) = \begin{cases} C_1\exp[(Le_F/2+\Lambda_F)x] - \frac{i}{c}Le_F e^{Le_F(x-\xi_f)}, & x < x_f \\ C_2\{\exp[(Le_F/2+\Lambda_F)x] - \exp[(Le_F/2-\Lambda_F)x]\}, & x > x_f, \end{cases}$$

$$w_{\mathrm{p}}(x)=\begin{cases} D_1\exp[(Le_{\mathrm{O}}/2+\Lambda_{\mathrm{O}})x], & x<x_{\mathrm{f}} \\ D_2\{\exp[(Le_{\mathrm{O}}/2+\Lambda_{\mathrm{O}})x]-\exp[(Le_{\mathrm{O}}/2-\Lambda_{\mathrm{O}})x]\} \\ +\frac{i}{c}(1+\phi^{-1})Le_{\mathrm{O}}\{\mathrm{e}^{Le_{\mathrm{O}}x}-\exp[(Le_{\mathrm{O}}/2-\Lambda_{\mathrm{O}})x]\}, & x>x_{\mathrm{f}}, \end{cases}$$

where

$$\Lambda_J=\frac{1}{2}\sqrt{Le_J^2+4iLe_Jc}, \quad J=T,F,O$$

with $Le_T=1$. The constants B_1,B_2,C_1,C_2,D_1 and D_2 are obtained by applying the jump and leakage conditions (21)–(24), which yield the inhomogeneous linear system

$$\begin{bmatrix} 1 & -1 & Le_{\mathrm{F}}^{-1} & -Le_{\mathrm{F}}^{-1} & 0 & 0 \\ 1 & -1 & 0 & 0 & Le_{\mathrm{O}}^{-1} & -Le_{\mathrm{O}}^{-1} \\ F_T & \frac{1}{2}-\Lambda_T & F_{\mathrm{F}} & \frac{1}{2}-Le_{\mathrm{F}}^{-1}\Lambda_{\mathrm{F}} & 0 & 0 \\ F_T & \frac{1}{2}-\Lambda_T & 0 & 0 & F_{\mathrm{O}} & \frac{1}{2}-Le_{\mathrm{O}}^{-1}\Lambda_{\mathrm{O}} \\ \frac{1-\gamma}{2}Le_{\mathrm{F}}b_{\mathrm{F}} & \frac{1+\gamma}{2}Le_{\mathrm{F}}b_{\mathrm{F}} & \frac{1-\gamma}{2}b_{\mathrm{F}}-1 & 0 & 0 & \frac{1+\gamma}{2}\frac{Le_{\mathrm{F}}}{Le_{\mathrm{O}}}b_{\mathrm{F}} \\ \frac{1-\gamma}{2}Le_{\mathrm{O}}b_{\mathrm{O}} & \frac{1+\gamma}{2}Le_{\mathrm{O}}b_{\mathrm{O}} & \frac{1-\gamma}{2}\frac{Le_{\mathrm{O}}}{Le_{\mathrm{F}}}b_{\mathrm{O}} & 0 & 0 & \frac{1+\gamma}{2}b_{\mathrm{O}}-1 \end{bmatrix} \times \begin{bmatrix} u_{\mathrm{p}}^+ \\ u_{\mathrm{p}}^- \\ v_{\mathrm{p}}^+ \\ v_{\mathrm{p}}^- \\ w_{\mathrm{p}}^+ \\ w_{\mathrm{p}}^- \end{bmatrix} = \frac{i}{c}\begin{bmatrix} 0 \\ 0 \\ q_3 \\ q_4 \\ 0 \\ 0 \end{bmatrix}, \tag{25}$$

where

$$F_J=-\frac{1}{2}+Le_J^{-1}\Lambda_J\coth(\Lambda_J\xi_{\mathrm{f}}), \quad J=T,F,O,$$

$$\begin{aligned} q_3=&(1/2-\Lambda_T)[1+(\Delta T-1)\mathrm{e}^{\xi_{\mathrm{f}}}]-(\Delta T-1)\mathrm{e}^{\xi_{\mathrm{f}}} \\ &\times[1/2-\Lambda_T\coth(\Lambda_T\xi_{\mathrm{f}})] \\ &-(\Delta T-1)\Lambda_T[1+\coth(\Lambda_T\xi_{\mathrm{f}})] \\ &\times\exp[(1/2-\Lambda_T)\xi_{\mathrm{f}}]-(1/2-Le_{\mathrm{F}}^{-1}\Lambda_{\mathrm{F}})Le_{\mathrm{F}}, \\ q_4=&(1/2-\Lambda_T)[1+(\Delta T-1)\mathrm{e}^{\xi_{\mathrm{f}}}]-(\Delta T-1)\mathrm{e}^{\xi_{\mathrm{f}}}[1/2-\Lambda_T\coth(\Lambda_T\xi_{\mathrm{f}})] \\ &-(\Delta T-1)\Lambda_T[1+\coth(\Lambda_T\xi_{\mathrm{f}})]\exp[(1/2-\Lambda_T)\xi_{\mathrm{f}}] \\ &-(1+\phi^{-1})Le_{\mathrm{O}}[1/2-Le_{\mathrm{O}}^{-1}\Lambda_{\mathrm{O}}\coth(\Lambda_{\mathrm{O}}\xi_{\mathrm{f}})]\mathrm{e}^{Le_{\mathrm{O}}\xi_{\mathrm{f}}} \\ &-(1+\phi^{-1})\mu_{\mathrm{O}}[1+\coth(\mu_{\mathrm{O}}\xi_{\mathrm{f}})]\exp[(Le_{\mathrm{O}}/2-\mu_{\mathrm{O}})\xi_{\mathrm{f}}], \end{aligned}$$

and $u_{\mathrm{p}}^+,u_{\mathrm{p}}^-,v_{\mathrm{p}}^+,v_{\mathrm{p}}^-,w_{\mathrm{p}}^+$ and w_{p}^- are the values of $u_{\mathrm{p}},v_{\mathrm{p}}$ and w_{p} at the oxidant and fuel sides of the flame sheet, respectively. The coefficient matrix in (25) depends on the four prescribed parameters $Le_{\mathrm{F}},Le_{\mathrm{O}},\phi$ and ΔT defining the combustion system, the imposed frequency c, and the Damköhler number Da. The amplitude and phase shift of forced oscillations for T,Y_{F} and Y_{O} at both sides of the flame sheet can be obtained from $u_{\mathrm{p}}^+,u_{\mathrm{p}}^-,v_{\mathrm{p}}^+,v_{\mathrm{p}}^-,w_{\mathrm{p}}^+$ and w_{p}^- by solving Eq. (25). However, under certain Damköhler numbers and forced frequencies, the determinant of the coefficient matrix in Eq. (25) could be zero, leading to infinitely large values of $u_{\mathrm{p}}^+,u_{\mathrm{p}}^-,v_{\mathrm{p}}^+,v_{\mathrm{p}}^-,w_{\mathrm{p}}^+$ and w_{p}^-, i.e. infinitely large amplitude of flame oscillations even under an $O(\varepsilon)$ weak forcing. This implies that resonance occurs under such an external forcing. The linear stability analysis performed by Kukuck and Matalon [18] for the intrinsic oscillation of the same flame yields a homogeneous linear system with the same coefficient matrix. The solvability condition, vanishing of the determinant of the coefficient matrix, produced the critical frequency and Damköhler number, c_0 and Da^*, corresponding to the marginally stable state. Thus, the imposed frequency and Damköhler number at resonance are identical to those at the onset of intrinsic oscillation, and hence the resonance occurs between the external forcing and intrinsic oscillation of the flame. Consequently, two conditions are required for the resonance of diffusion flame to occur: the flame is close to the stability boundary, i.e., $Da\to Da^*$, and the imposed frequency c approaches the critical frequency c_0.

The inhomogeneous system (25) gives the dependence of the amplitude and phase shifts of forced oscillation on the imposed frequency c and the Damköhler number Da. Fig. 2 shows the amplitude of u_{p}^+ versus the imposed frequency c for different values of Da. It is seen that when the flame is at the instability boundary, i.e. $Da=Da^*$, the imposed velocity fluctuation induces infinitely large flame oscillations, i.e. resonance, as c approaches c_0. For Da sufficiently larger than Da^*, the oscillation amplitude decreases monotonically with increasing c, while for Da close enough to Da^*, the oscillation amplitude peaks at the frequency close to but smaller than the natural frequency c_0. This differs from previous investigations that predicted only the monotonic attenuation of forced oscillation with the increase of the imposed frequency. Now we know that this monotonic dependence holds only when the flame is sufficiently away from the unstable state so that the resonance between the external forcing and intrinsic oscillation of flame does not occur. Fig. 3 shows variations of the phase shifts of $u_{\mathrm{p}}^+,u_{\mathrm{p}}^-,v_{\mathrm{p}}^+,v_{\mathrm{p}}^-,w_{\mathrm{p}}^+$ and w_{p}^- with the Damköhler number Da for $c=c_0$. It is seen that the oscillation of reactant leakages v_{p}^+ and w_{p}^- are always in phase. As Da approaches Da^*, i.e. the flame approaches the resonance condition, temperature oscillations on both sides of the flame sheet, u_{p}^+ and u_{p}^-, become in phase and the oscillations of the mass fractions of fuel and oxidant on both

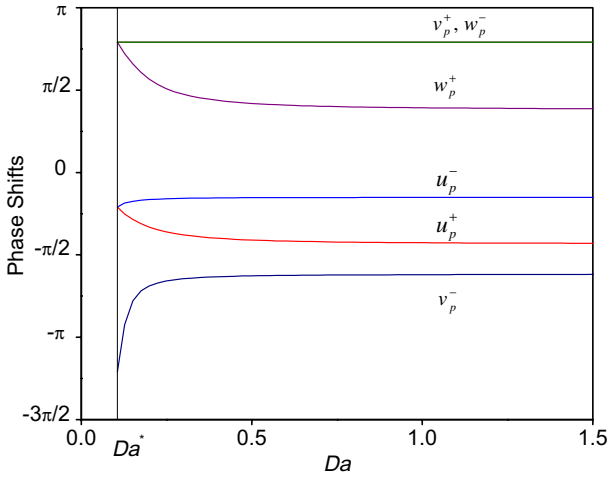

Fig. 3. Phase shifts of $u_{\mathrm{p}}^+,u_{\mathrm{p}}^-,v_{\mathrm{p}}^+,v_{\mathrm{p}}^-,w_{\mathrm{p}}^+$ and w_{p}^- versus Da with $c=c_0$.

sides of the flame sheet, $v_{\rm p}^+, v_{\rm p}^-, w_{\rm p}^+$ and $w_{\rm p}^-$, become in phase as well. The phase difference between the oscillations of temperature, $u_{\rm p}^+$ and $u_{\rm p}^-$, and mass fractions, $v_{\rm p}^+, v_{\rm p}^-, w_{\rm p}^+$ and $w_{\rm p}^-$, is π when the flame is at resonance, indicating they are out of phase. This is because higher flame temperatures lead to less reactant leakages, and vice versa.

4. Nonlinear response

The preceding analysis predicts infinite oscillation amplitude at the resonant frequency. However, the amplitude is expected to be limited by the inherent nonlinearities in the problem. Here we derive an evolution equation for the amplitude of forced oscillation near resonance. We adopt the scalings:

$$\begin{aligned} &h = \varepsilon^2, \\ &(Da - Da^*)/Da^* = \varepsilon^2, \\ &(c - c_0)/c_0 = \omega\varepsilon^2, \end{aligned} \tag{26}$$

so that the flame oscillation exhibits a weakly nonlinear characteristic and a long time transient behavior. Thus we introduce the "slow time" variables

$$\tau_1 = \varepsilon t, \quad \tau_2 = \varepsilon^2 t,$$

associated with the long time transient behavior. The velocity fluctuation $H(t)$ can be rewritten as

$$H(t) = \varepsilon^3 \exp(ic_0\tau) + \text{c.c.},$$

where $\tau = t + \omega\tau_2$.

We expand the variables $u_{\rm p}, v_{\rm p}$ and $w_{\rm p}$ in a power series in ε,

$$(u_{\rm p}, v_{\rm p}, w_{\rm p}) = \sum_{m=0}^{\infty} (u_m, v_m, w_m)\varepsilon^m,$$

and expand the governing equations, boundary, jump and leakage conditions for u, v and w (17)–(24) in terms of ε. We obtain a system of equations to be solved at each order:

$$L\begin{pmatrix} u_m \\ v_m \\ w_m \end{pmatrix} = \begin{pmatrix} \frac{\partial^2 u_m}{\partial x^2} - \frac{\partial u_m}{\partial x} - \frac{\partial u_m}{\partial t} \\ \frac{\partial^2 v_m}{\partial x^2} - Le_{\rm F}\frac{\partial v_m}{\partial x} - Le_{\rm F}\frac{\partial v_m}{\partial t} \\ \frac{\partial^2 w_m}{\partial x^2} - Le_{\rm O}\frac{\partial w_m}{\partial x} - Le_{\rm O}\frac{\partial w_m}{\partial t} \end{pmatrix} = \begin{pmatrix} p_m \\ q_m \\ r_m \end{pmatrix}, \tag{27}$$

with the boundary conditions:

$$u_m = v_m = w_m = 0 \quad \text{at } x = 0 \quad \text{and as } x \to -\infty, \tag{28}$$

jump conditions:

$$[u_m] = -Le_{\rm F}^{-1}[v_m] = -Le_{\rm O}^{-1}[w_m], \tag{29}$$

$$\left[u_m - \frac{\partial u_m}{\partial x}\right] = -\left[v_m - Le_{\rm F}^{-1}\frac{\partial v_m}{\partial x}\right] = -\left[w_m - Le_{\rm O}^{-1}\frac{\partial w_m}{\partial x}\right], \tag{30}$$

and leakage conditions:

$$\left(\frac{1-\gamma}{2}Le_{\rm F}b_{\rm F}\right)u_m^+ + \left(\frac{1+\gamma}{2}Le_{\rm F}b_{\rm F}\right)u_m^- + \left(\frac{1-\gamma}{2}b_{\rm F} - 1\right)v_m^+ + \left(\frac{1+\gamma}{2}\frac{Le_{\rm F}b_{\rm F}}{Le_{\rm O}}\right)w_m^- = \alpha_{{\rm F}m}, \tag{31}$$

$$\left(\frac{1-\gamma}{2}Le_{\rm O}b_{\rm O}\right)u_m^+ + \left(\frac{1+\gamma}{2}Le_{\rm O}b_{\rm O}\right)u_m^- + \left(\frac{1-\gamma}{2}\frac{Le_{\rm O}b_{\rm O}}{Le_{\rm F}}\right)v_m^+ + \left(\frac{1+\gamma}{2}b_{\rm O} - 1\right)w_m^- = \alpha_{{\rm O}m}, \tag{32}$$

where $m = 0, 1, 2, \ldots$ and

$$b_j = \delta_{\rm b}^* \frac{\partial S_j(\gamma, \delta_{\rm b}^*)}{\partial \delta_{\rm b}}, \quad j = F, O,$$

with $\delta_{\rm b}^*$ being the critical reduced Damköhler number at the marginally stable state. Note that the only non-linearity arises in the leakage conditions (31) and (32) from the nonlinear chemical kinetics.

At leading order $m = 0$, $p_0 = q_0 = r_0 = \alpha_{\rm F0} = \alpha_{\rm O0} = 0$, and we recover the homogeneous linear problem, such that the solutions are given as

$$(u_0, v_0, w_0) = \begin{cases} A(\tau_1, \tau_2)\Phi_J^-(x)\exp(ic_0\tau) + \text{c.c.}, & x < x_{\rm f}, \\ A(\tau_1, \tau_2)\Phi_J^+(x)\exp(ic_0\tau) + \text{c.c.}, & x > x_{\rm f}, \end{cases} \tag{33}$$

where $J = T, F, O$ corresponds to the solutions of u_0, v_0 and w_0, respectively, and

$$\begin{aligned} &\Phi_J^-(x) = C_J^- \exp[(Le_J/2 + \lambda_J)x], \\ &\Phi_J^+(x) = C_J^+\{\exp[(Le_J/2 + \lambda_J)x] - \exp[(Le_J/2 - \lambda_J)x]\}, \\ &\lambda_J = \frac{1}{2}\sqrt{Le_J^2 + 4iLe_Jc_0}. \end{aligned}$$

The constants $C_J^{\pm}$ are determined by the linear system (A1) given in the appendix of Ref. [21], derived from relating the solutions of u_0, v_0 and w_0 through the jump and leakage conditions. The amplitude function $A(\tau_1, \tau_2)$, which is a function of the slow time variables, τ_1 and τ_2, is determined by going to higher orders in our scheme. This procedure is the same as that in Ref. [21] and hence will not be repeated here. At each order, solutions exist only if appropriate solvability conditions are satisfied. The solvability condition for u_1, v_1 and w_1 yields $\partial A/\partial\tau_1 = 0$. Thus, the amplitude function A is actually only a function of the slow time variable τ_2.

At $O(\varepsilon^2)$, the inhomogeneous terms in Eqs. (27),(31) and (32) are:

$$\begin{aligned} &p_2 = (A' + ic_0\omega A)\phi_T + (T_0)_x, \\ &q_2 = Le_{\rm F}(A' + ic_0\omega A)\phi_{\rm F} + (Y_{F,0})_x, \\ &r_2 = Le_{\rm O}(A' + ic_0\omega A)\phi_{\rm O} + (Y_{O,0})_x, \\ &\alpha_{j2} = \alpha_{j2,3}A^3\exp(3ic_0t) + (\alpha_{j2,2}A|A|^2 + \alpha_{j2,1}A)\exp(ic_0t) + \text{c.c.}, \end{aligned}$$

where the prime of A denotes differentiation with respect to τ_2,

$$\alpha_{j2,1} = sb_{j1}F(\Phi),$$
$$\alpha_{j2,2} = b_{j1}(F(\Phi)F(\Omega)+\overline{F}(\Phi)F(\Theta))+b_{j2}F(\Phi)|F(\Phi)|^2,$$
$$\alpha_{j2,3} = b_{j1}F(\Phi)F(\Theta)+\frac{1}{3}b_{j2}F^3(\Phi),$$
$$s = \frac{s'}{1-\left(\frac{1-\gamma}{2}-Le_F\frac{1-e^{\xi_f}}{1-e^{Le_F\xi_f}}+\frac{1+\gamma}{2}\frac{Le_F}{Le_O}\frac{1-e^{Le_O\xi_f}}{1-e^{Le_F\xi_f}}\right)b_F},$$
$$b_{j1} = -Le_j\left\{\delta_b^*\frac{\partial S_j(\gamma,\delta_b^*)}{\partial\delta_b}+\delta_b^{*2}\frac{\partial^2 S_j(\gamma,\delta_b^*)}{\partial\delta_b^2}\right\},$$
$$b_{j2} = -Le_j\left\{\frac{\delta_b^*}{2}\frac{\partial S_j(\gamma,\delta_b^*)}{\partial\delta_b}+\frac{3\delta_b^{*2}}{2}\frac{\partial^2 S_j(\gamma,\delta_b^*)}{\partial\delta_b^2}+\frac{\delta_b^{*3}}{2}\frac{\partial^3 S_j(\gamma,\delta_b^*)}{\partial\delta_b^3}\right\},$$
$$\Theta_J^-(x) = D_J^-\exp[(Le_J/2+\mu_J)x],$$
$$\Theta_J^-(x) = D_J^-\{\exp[(Le_J/2+\mu_J)x]-\exp[(Le_J/2+\mu_J)x]\},$$
$$\Omega_J^-(x) = B_J^-e^{Le_Jx},$$
$$\Omega_J^+(x) = B_J^+(1-e^{Le_Jx}),$$
$$\mu_J = \frac{1}{2}\sqrt{Le_J^2+8iLe_Jc_0},$$

and the function $F(\Phi)$ is defined as

$$F(\Phi) = \frac{1+\gamma}{2}\{\Phi_T^-(\xi_f)+Le_O^{-1}\Phi_O^-(\xi_f)\}+\frac{1-\gamma}{2}\{\Phi_T^+(\xi_f)+Le_F^{-1}\Phi_F^+(\xi_f)\},$$

and the overbar designates the complex conjugate. The constants $B_J^\pm$ and $D_J^\pm$ are determined by the linear systems (A3) and (A4), respectively, given in the appendix of [21]. Applying the solvability condition at this order yields

$$A'+(s\alpha_1+ic_0\omega)A+\alpha_2A|A|^2+\alpha_3 = 0, \tag{34}$$

where the coefficients are given by

$$\alpha_1 = \frac{\alpha_{10}}{\alpha_0},\quad \alpha_2 = \frac{\alpha_{20}}{\alpha_0},\quad \alpha_3 = \frac{\alpha_{30}}{\alpha_0},$$
$$\alpha_0 = \int_{-\infty}^{\xi_f}[\overline{\Psi}_T^-\phi_T^-+Le_F\overline{\Psi}_F^-\phi_F^-+Le_O\overline{\Psi}_O^-\phi_O^-]\,dx+\int_{\xi_f}^{0}[\overline{\Psi}_T^+\phi_T^++Le_F\overline{\Psi}_F^+\phi_F^++Le_O\overline{\Psi}_O^+\phi_O^+]\,dx,$$
$$\alpha_{10} = \left\{\left(\frac{1-\gamma}{2\chi}\frac{b_F}{Le_Ob_O}+1\right)\left[\frac{d\overline{\Psi}_F}{dx}\right]+\left(\frac{1-\gamma}{2\chi}\frac{1}{Le_F}\right)\left[\frac{d\overline{\Psi}_O}{dx}\right]\right\}\alpha_{F2,1}+\left\{\left(\frac{1+\gamma}{2\chi}\frac{Le_Fb_F}{Le_O^2b_O}\right)\left[\frac{d\overline{\Psi}_F}{dx}\right]-\frac{1}{\chi}\left(\frac{1-\gamma}{2}b_F-1\right)\frac{1}{Le_Ob_O}\left[\frac{d\overline{\Psi}_O}{dx}\right]\right\}\alpha_{O2,1},$$
$$\alpha_{20} = \left\{\left(\frac{1-\gamma}{2\chi}\frac{b_F}{Le_Ob_O}+1\right)\left[\frac{d\overline{\Psi}_F}{dx}\right]+\left(\frac{1-\gamma}{2\chi}\frac{1}{Le_F}\right)\left[\frac{d\overline{\Psi}_O}{dx}\right]\right\}\alpha_{F2,2}+\left\{\left(\frac{1+\gamma}{2\chi}\frac{Le_Fb_F}{Le_O^2b_O}\right)\left[\frac{d\overline{\Psi}_F}{dx}\right]-\frac{1}{\chi}\left(\frac{1-\gamma}{2}b_F-1\right)\frac{1}{Le_Ob_O}\left[\frac{d\overline{\Psi}_O}{dx}\right]\right\}\alpha_{O2,2},$$
$$\alpha_{30} = \int_{-\infty}^{\xi_f}[\overline{\Psi}_T^-(T_0^-)_x+Le_F\overline{\Psi}_F^-(Y_{F,0}^-)_x+Le_O\overline{\Psi}_O^-(Y_{O,0}^-)_x]\,dx+\int_{\xi_f}^{0}[\overline{\Psi}_T^+(T_0^+)_x+Le_F\overline{\Psi}_F^+(Y_{F,0}^+)_x+Le_O\overline{\Psi}_O^+(Y_{O,0}^+)_x]\,dx,$$
$$\Psi_J^-(x) = E_J^-\exp[(-Le_J/2+\bar{\lambda}_J)x]$$
$$\Psi_J^+(x) = E_J^+\{\exp[(-Le_J/2+\bar{\lambda}_J)x]-\exp[(-Le_J/2-\bar{\lambda}_J)x]\},$$

and the constants $E_J^\pm$ are determined by the linear system (A2) given in the appendix of [21].

Note that the amplitude function A is complex and hence includes the information of both amplitude and phase. We construct solutions by first writing the amplitude function A in the polar form and separating α_1,α_2, and α_3 into their real and imaginary parts:

$$A = R(\tau_2)\exp[i\theta(\tau_2)],$$
$$\alpha_1 = \alpha_{1r}+i\alpha_{1i},\quad \alpha_2 = \alpha_{2r}+i\alpha_{2i},\quad \alpha_3 = \alpha_{3r}+i\alpha_{3i}, \tag{35}$$

where R is the amplitude and θ the polar angle indicating phase shift. The complex evolution Eq. (33) can now be expressed as two real equations, for the amplitude and the phase shift:

$$R'+s\alpha_{1r}R+\alpha_{2r}R^3+\alpha_{3r}\cos\theta+\alpha_{3i}\sin\theta = 0, \tag{36}$$
$$R\theta'+(s\alpha_{1i}+c_0\omega)R+\alpha_{2i}R^3+\alpha_{3i}\cos\theta-\alpha_{3r}\sin\theta = 0. \tag{37}$$

We note that the evolution Eqs. (34) or (36) and (37) have a similar form as those describing nonlinear oscillators, e.g. the Van der Pol oscillator, under weak damping and forcing [22]. A simple comparison of these systems shows that the term $s\alpha_1$ in Eqs. (34) and (36), which quantifies the deviation of Da from Da^*, plays the role of damping for the forced flame oscillation.

Here, we study the steady-state solutions of Eqs. (36) and (37) in order to assess the final amplitude and phase of the forced flame oscillation under external forcing. Combining the steady-state forms of Eqs. (36) and (37) yields the following cubic equation for R^2.

$$R^6+\frac{2[s(\alpha_{1r}\alpha_{2r}+\alpha_{1i}\alpha_{2i})+c_0\omega\alpha_{2i}]}{|\alpha_2|^2}R^4+\frac{(s\alpha_{1r})^2+(s\alpha_{1i}+c_0\omega)^2}{|\alpha_2|^2}R^2-\frac{|\alpha_3|^3}{|\alpha_2|^2} = 0. \tag{38}$$

Eq. (38) will possess three real and positive solutions whenever the following inequality is satisfied:

$$\left|\frac{\alpha_{2i}}{\alpha_{2r}}\right| \geqslant \sqrt{3}. \tag{39}$$

It has a single real solution otherwise. We now consider the dependence of α_2 on the four prescribed parameters, Le_F, Le_O, ϕ and ΔT. In Fig. 4 we plot its variations with each prescribed parameter to determine conditions (if any) for which the inequality in (39) is satisfied, which would indicate multiplicity of solutions. The green lines in each figure show the transition boundary at which $|\alpha_{2i}/\alpha_{2r}| = \sqrt{3}$. As seen in Fig. 4, we have found that for a wide range of realistic parameter values, all curves lie to the left of the transition boundary, indicating that solutions to (36) and (37) are single valued.

We now investigate the sensitivity of flames to the imposed velocity fluctuations under different prescribed parameters through this single-valued solution. Fig. 5 shows variation of the amplitude of forced oscillation, R, with the normalized frequency ω, defined in Eq. (26), for

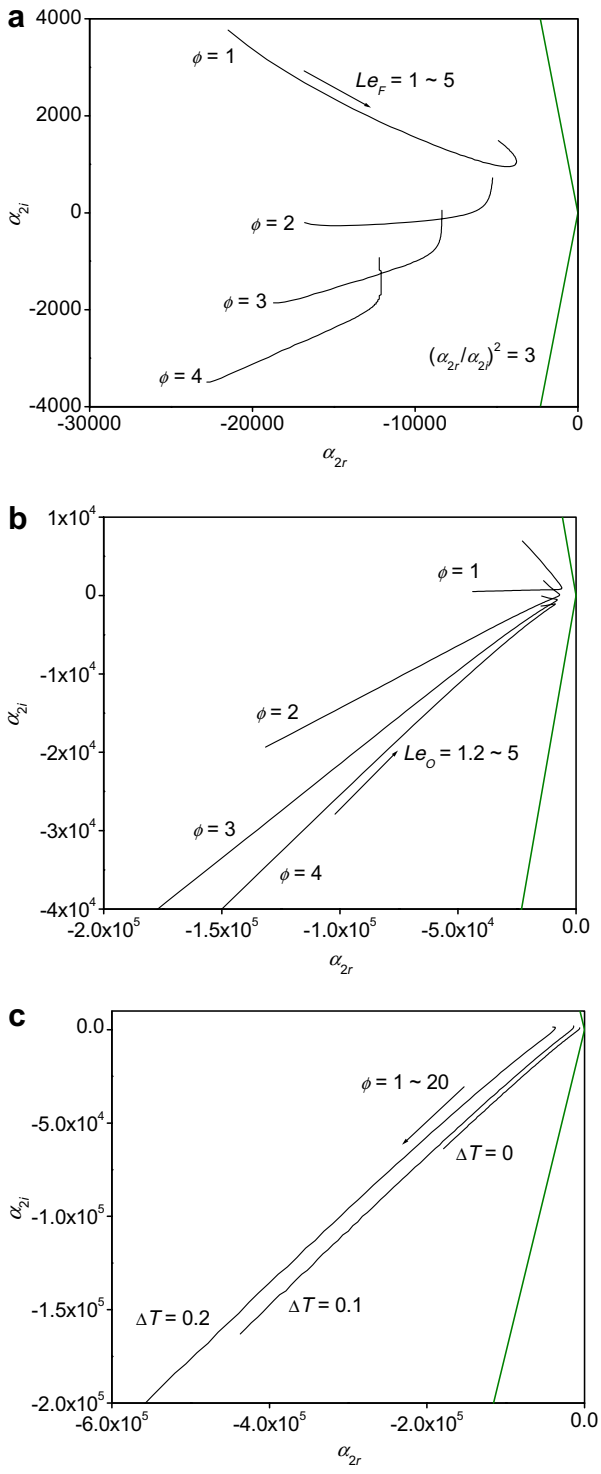

Fig. 4. Variations of α_2 (a) with Le_F for different ϕ with $Le_O = 2$ and $\Delta T = 0$, (b) with Le_O for different ϕ with $Le_F = 2$ and $\Delta T = 0$, and (c) with ϕ for different ΔT with $Le_F = Le_O = 2$.

$Da = Da^*, Le_F = 2, Le_O = 2, \phi = 1$ and $\Delta T = 0$. It is seen that the dependence of R on the imposed frequency shows similar behavior as those in Fig. 2 for Da slightly larger than Da^*, in that it peaks at the frequency close to but slightly smaller than the intrinsic flame oscillation frequency c_0. The finite amplitude of forced oscillation at

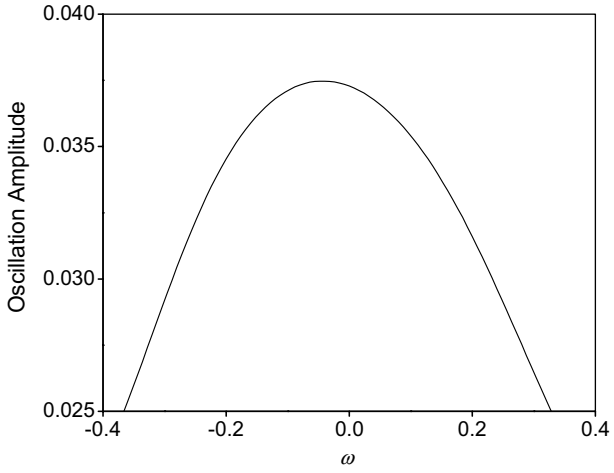

Fig. 5. Variation of oscillation amplitude R with the normalized imposed frequency for $Da = Da^*$ (with $Le_F = 2$, $Le_O = 2$, $\phi = 1$ and $\Delta T = 0$).

the resonance condition, i.e. $Da = Da^*$ and $c = c_0$, is due to the nonlinear effects considered through the nonlinear analysis. We hence can plot the dependence of this peak amplitude, R_{max}, on the system parameters such as Le_F, Le_O, ϕ and ΔT to examine at what conditions the flame is able to achieve the largest R_{max} and hence is most responsive to the external forcing. Since the maximum amplitude of forced oscillation is achieved under the smallest damping, R_{max} can be solved from Eq. (38) by setting the damping effect $s = 0$, as $R_{max} = (\alpha_3/\alpha_{2r})^{1/3}$, which can be derived to occur at the normalized frequency $\omega = -\alpha_{2i}\ (\alpha_3/\alpha_{2r})^{2/3}$. Thus, due to the nonlinearity, the flame oscillates with the maximum amplitude at the imposed frequency not necessarily equal to the natural frequency, c_0. Whether the maximum amplitude, R_{max}, occurs at the frequency smaller or larger than c_0 depends on the sign of α_{2i}, which in turn depends on the prescribed parameters. The peaking of the curves at $c < c_0$ shown in Figs. 2 and 5 is due to the parameters we have used, $Le_F = 2, Le_O = 2, \phi = 1$ and $\Delta T = 0$ that yield a positive α_{2i}. Fig. 6 shows variations of R_{max} with Le_F for different values of ϕ. It is seen that except for $\phi = 1, R_{max}$ increases monotonically with Le_F. In fact, R_{max} peaks at a much larger Le_F, e.g. $Le_F = 14.4$ for $\phi = 3$, which is out of the range of this plot. Since for most hydrocarbon–air diffusion flames $\phi > 1$ and fuels with such large Lewis number are rare, it can be considered that R_{max} increases with Le_F monotonically. Thus, in general the flame is more sensitive to the external forcing for larger Le_F. Fig. 7 shows variations of R_{max} with Le_O for different values of ϕ. It is seen that for $\phi > 1$ most of the $R_{max} \sim Le_O$ curves peak within the range of $1 < Le_O < 2$, which is a more practical range for the oxidant. Thus, flames with Le_O falling in this range are most responsive to the external forcing. Furthermore, it is seen from Figs. 6 and 7 that except for smaller Le_O where R_{max} is not sensitive to ϕ, R_{max} decreases with increasing ϕ over most of the parameter range for Le_F and Le_O. Fig. 8 shows the variations of R_{max} with ϕ for different values of

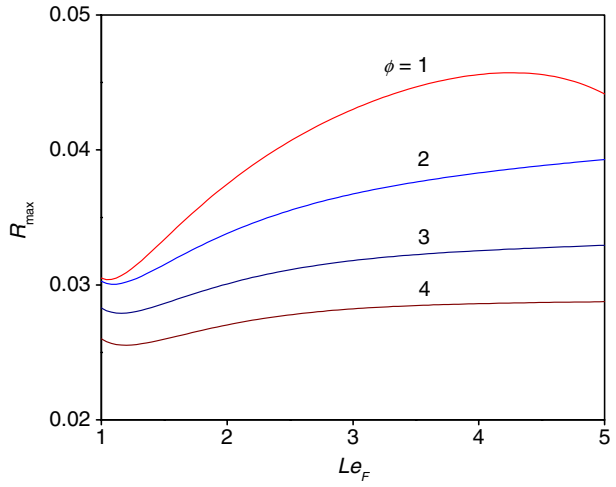

Fig. 6. Variations of the maximum oscillation amplitude R_{max} with Le_F for different ϕ (with $Le_O = 2$ and $\Delta T = 0$).

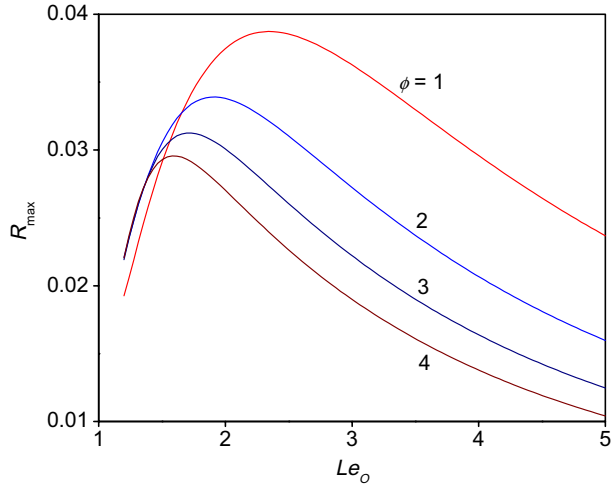

Fig. 7. Variations of the maximum oscillation amplitude R_{max} with Le_O for different ϕ (with $Le_F = 2$ and $\Delta T = 0$).

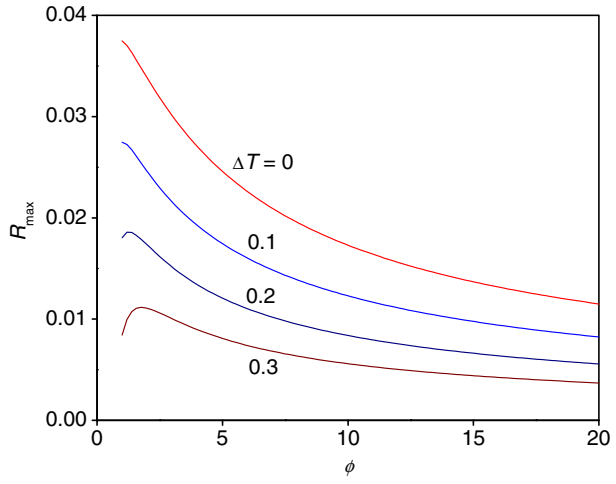

Fig. 8. Variations of the maximum oscillation amplitude R_{max} with ϕ for different ΔT (with $Le_F = 2$ and $Le_O = 2$).

ΔT. It is seen that R_{max} decreases monotonically with increasing ϕ over most of its range except for larger ΔT and small ϕ, under which R_{max} increases with increasing ϕ over a very narrow range of ϕ. Thus, flames with smaller ϕ, in general, are more responsive to the external forcing.

5. Conclusions

The response of flame oscillations to external velocity fluctuations of small amplitude is examined. An analysis on the linear response is first conducted and the results show that when the flame is near the boundary of thermal–diffusive pulsating instability, the velocity fluctuation may induce resonance as the fluctuation frequency approaches the natural frequency of the intrinsic oscillation. Thus, the amplitude–frequency response curve exhibits a peak around the natural frequency. Monotonic dependence of the oscillation amplitude on the forced frequency holds only when the flame is sufficiently away from resonance. A nonlinear near-resonant response is then conducted to study the effects of inherent nonlinearities on the response of flame oscillation by deriving an evolution equation for the amplitude of forced oscillation. Examination of the derived evolution equation reveals that, in most situations, flames with larger Le_F, smaller ϕ and ΔT, and $1 < Le_O < 2$ have the largest oscillation amplitude at resonance. Thus, these flames are most responsive to the external forcing.

Acknowledgement

The support of the Air Force Office of Scientific Research is gratefully acknowledged.

References

[1] N. Peters, Laminar flamelet concepts in turbulent combustion, Proc. Combust. Inst. 21 (1987) 1231–1250.
[2] W.C. Strahle, Periodic solutions to a convective droplet burning problem: stagnation point, Proc. Combust. Inst. 10 (1965) 1783–1792.
[3] T. Saitoh, Y. Otsuka, Unsteady behavior of diffusion flames and premixed flames for counter flow geometry, Combust. Sci. Technol. 12 (1976) 135–146.
[4] N. Darabiha, Transient behavior of laminar counterflow hydrogen–air diffusion with complex chemistry, Combust. Sci. Technol. 86 (1992) 163–181.
[5] V.R. Katta et al., Extinction criterion for unsteady, opposing-jet diffusion flames, Combust. Flame 137 (2004) 198–221.
[6] J.S. Kistler et al., Extinction of counterflow diffusion flames under velocity oscillations, Proc. Combust. Inst. 26 (1996) 113–120.
[7] T.M. Brown, R.M. Pitz, C.J. Sung, Oscillatory stretch effects on the structure and extinction of counterflow diffusion flames, Proc. Combust. Inst. 27 (1998) 703–710.
[8] R.K. Mohammed, M.A. Tanoff, M.D. Smooke, A.M. Schaffer, Computational and experimental study of a forced, time-varying, axisymmetric, laminar diffusion flame, Proc. Combust. Inst. 27 (1998) 693–702.
[9] F.N. Egolfopoulos, C.S. Campbell, Unsteady counterflowing strained diffusion flames: diffusion-limited frequency response, J. Fluid Mech. 318 (1996) 1–29.

[10] E.J. Welle et al., The response of a propane-air counter-flow diffusion flame subjected to a transient flow field, Combust. Flame 135 (2003) 285–297.
[11] F.N. Egolfopoulos, Structure and extinction of unsteady, counter-flowing, strained, non-premixed flames, Int. J. Energy Res. 24 (2000) 989–1010.
[12] B. Cuenot, F.N. Egolfopoulos, T. Poinsot, An unsteady laminar flamelet model for non-premixed combustion, Combust. Theory Model. 4 (2000) 77–97.
[13] H.G. Im, C.K. Law, J.S. Kim, F.A. Williams, Response of counter-flow diffusion flames to oscillating strain rates, Combust. Flame 100 (1995) 21–30.
[14] H.G. Im, J.K. Bechtold, C.K. Law, Counterflow diffusion flames with unsteady strain rates, Combust. Sci. Technol. 106 (1995) 345–361.
[15] W. Chan, J. T'ien, An experiment on spontaneous flame oscillation prior to extinction, Combust. Sci. Technol. 18 (1978) 139–143.
[16] V. Nayagam, F.A. Williams, Dynamics of diffusion flame oscillations prior to extinction during low gravity droplet combustion, in: Seventh International Conference on Numerical Combustion, New York, 1998, p. 46.
[17] M. Furi, P. Papas, P.A. Monkewitz, Non-premixed jet flame pulsations near extinction, Proc. Combust. Inst. 28 (2000) 831–838.
[18] S. Kukuck, M. Matalon, The onset of oscillations in diffusion flames, Combust. Theory Model. 5 (2001) 217–240.
[19] S. Cheatham, M. Matalon, A general asymptotic theory of diffusion flames with application to cellular instability, J. Fluid Mech. 414 (2000) 105–144.
[20] A. Liñán, The asymptotic structure of counterflow diffusion flames for large activation energies, Acta Astronaut. 1 (1974) 1007–1039.
[21] H.Y. Wang, J.K. Bechtold, C.K. Law, Nonlinear oscillations in diffusion flames, Combust. Flame 145 (2006) 376–389.
[22] J. Kevorkian, J.D. Cole, Perturbation Methods in Applied Mathematics, Springer, New York, 1981, pp. 141–151.